

Loss of Drs2p Does Not Abolish Transfer of Fluorescence-labeled Phospholipids across the Plasma Membrane of *Saccharomyces cerevisiae**

(Received for publication, March 27, 1998, and in revised form, August 4, 1998)

Anja Siegmund‡§, Althea Grant¶, Cesar Angeletti¶, Lynn Malone¶, J. Wylie Nichols¶, and Hans K. Rudolph‡¶||

From the ‡Institut für Biochemie der Universität Stuttgart, Pfaffenwaldring 55, D-70569 Stuttgart, Germany and ¶Department of Physiology, Emory University School of Medicine, Atlanta, Georgia 30322

The yeast *DRS2* gene, which is required for growth at 23 °C or below, encodes a member of a P-type ATPase subgroup reported to transport aminophospholipids between the leaflets of the plasma membrane. Here, we evaluated the potential role of Drs2p in phospholipid transport. When examined by fluorescence microscopy, a *drs2* null mutant showed no defect in the uptake or distribution of fluorescently labeled 1-palmitoyl-2-[6-(7-nitrobenz-2-oxa-1,3-diazol-4-yl (NBD))aminocaproyl]phosphatidylserine or 1-myristoyl-2-[6-NBD-aminocaproyl]phosphatidylethanolamine. Quantification of the amount of cell-associated NBD fluorescence using flow cytometry indicated a significant decrease in the absence of Drs2p, but this decrease was not restricted to the aminophospholipids (phosphatidylserine and phosphatidylethanolamine) and was dependent on culture conditions. Furthermore, the absence of Drs2p had no effect on the amount of endogenous PE exposed to the outer leaflet of the plasma membrane as detected by labeling with trinitrobenzene sulfonic acid. The steady state pool of Drs2p, which was shown to reside predominantly in the plasma membrane, increased upon shift to low temperature or exposure to various divalent cations (Mn^{2+} , Co^{2+} , Ni^{2+} , and Zn^{2+} but not Ca^{2+} or Mg^{2+}), conditions that also inhibited the growth of a *drs2* null mutant. The data presented here call into question the identification of Drs2p as the exclusive or major aminophospholipid translocase in yeast plasma membranes (Tang, X., Halleck, M. S., Schlegel, R. A., and Williamson, P. (1996) *Science* 272, 1495–1497).

Most biological membranes appear to possess a nonrandom distribution of phospholipids between the two leaflets of the bilayer (1). An asymmetric organization of phospholipids, in which phosphatidylethanolamine (PE)¹ and phosphatidyl-

serine (PS) are enriched in the inner leaflet facing the cytoplasm, and phosphatidylcholine (PC), sphingomyelin, and glycolipids are predominantly located on the outer leaflet, has been well documented for the plasma membranes of numerous cell types (2, 3). The loss of this asymmetric distribution and the resulting appearance of PS at the cell surface triggers a variety of intercellular communication and signaling processes, such as platelet activation (4), clearance of senescent red cells (5), and phagocytosis of apoptotic cells (6, 7). However, the establishment and regulation of this asymmetric distribution as well as its physiological function in single cells are poorly understood. It is generally thought that the transbilayer movement ("flip-flop") of phospholipids is mediated by ATP-dependent flippases, and several proteins with flippase activity have been identified in mammalian cells. The ABC transporters, human MDR1 and MDR3 (8, 9), mouse *mdr2* (10), and yeast *Pdr5p* and *Yor1p* (11) have been shown to exhibit outward-directed phospholipid flippase activity.

A recent report on the cloning of a flippase from bovine chromaffin granules has implicated a novel subgroup within the P-type ATPase family in the inward-directed transport of aminophospholipids (12). Most P-type ATPases, represented by a group of 18 genes in the genome of the yeast *Saccharomyces cerevisiae* (13), are biochemically well characterized and known to function in the transport of mono- or divalent cations (14). The Na^+/K^+ ATPases, various Ca^{2+} ATPases of animal cells as well as the H^+ -ATPases of fungi and plants belong to this family of ion transporters, which share a characteristic set of conserved regions and a similar transmembrane topology (14). The members of the new subgroup differ from the ion-transporting ATPases in several amino acids within transmembrane segments critically involved in ion translocation. Apart from the bovine cDNA, the yeast *DRS2* gene and four related yeast genes (13) as well as sequences from *Plasmodium falciparum* and *Caenorhabditis elegans* appear to carry these changes (12) whereby negatively charged residues have been replaced by bulky, hydrophobic groups. The observation of a defect in fluorescently labeled PS (P-C₆-NBD-PS) internalization in a *drs2* mutant at low temperature has been interpreted as evidence for the biochemical function of this group of enzymes as aminophospholipid translocases (12).

In this report, we examined the potential role of Drs2p in phospholipid transport using fluorescence microscopy, flow cytometry, and TNBS labeling. The deletion of *DRS2* had no effect on the uptake or distribution of fluorescently labeled PS (P-C₆-NBD-PS) or PE (M-C₆-NBD-PE) detected by fluorescence

* This work was supported by the BMFT Zentrales Schwerpunktprojekt Bioverfahrenstechnik, Universität Stuttgart (to H. K. R.) and National Institutes of Health Grant GM52410 (to J. W. N.). The costs of publication of this article were defrayed in part by the payment of page charges. This article must therefore be hereby marked "advertisement" in accordance with 18 U.S.C. Section 1734 solely to indicate this fact.

§ Recipient of a stipend from the Landesgraduierten-Förderung (Universität Stuttgart).

|| To whom correspondence should be addressed. Tel.: +49 711-685-4389; Fax: (+49 711-685-4392); E-mail: rudolph@po.uni-stuttgart.de.

¹ The abbreviations used are: PE, phosphatidylethanolamine; PS, phosphatidylserine; PC, phosphatidylcholine; TNBS, trinitrobenzene sulfonic acid; NBD, 7-nitrobenz-2-oxa-1,3-diazol-4-yl; M-C₆-NBD-PC, 1-myristoyl-2-[6-NBD-aminocaproyl]phosphatidylcholine; M-C₆-NBD-PE, 1-myristoyl-2-[6-NBD-aminocaproyl]phosphatidylethanolamine; P-C₆-NBD-PS, 1-palmitoyl-2-[6-NBD-aminocaproyl]phosphatidylserine; HA, hemagglutinin; kb, kilobase(s); YPAD, yeast extract/peptone/ade-

nine/glucose; DOPC, dioleoylphosphatidylcholine; N-Rh-DOPE, N-rhodamine-dioleoylphosphatidyl ethanol amine; SDC, synthetic-complete glucose; YDP, yeast extract/peptone/glucose.

microscopy. Quantification of the amount of cell-associated NBD fluorescence indicated a significant decrease in the absence of Drs2p, but this decrease was not exclusive to the aminophospholipids (PE and PS) and was dependent on culture conditions. The absence of Drs2p had no effect on the amount of endogenous PE exposed to the outer leaflet of the plasma membrane as detected by labeling with TNBS. The steady state pool of Drs2p, which was shown to reside predominantly in the plasma membrane, increased upon shift to low temperature or exposure to various heavy metal cations, conditions that inhibited the growth of a *drs2* null mutant. The data presented here call into question the identification of Drs2p as the exclusive or major aminophospholipid translocase in yeast plasma membranes (12).

EXPERIMENTAL PROCEDURES

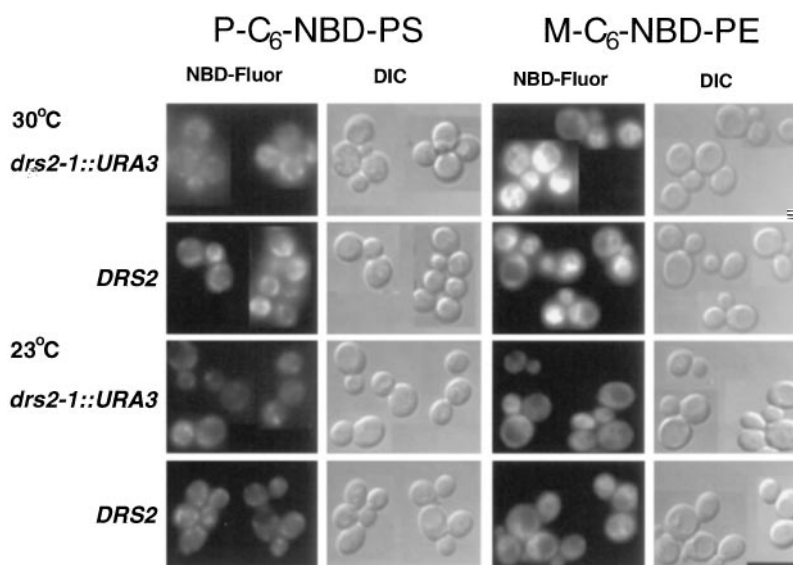
Yeast Strains and Growth Conditions—All yeast strains used in this study were derived from the S288C-related wild-type strain YR98 (*MAT α ade2 his3- Δ 200 leu2-3, 112 lys2- Δ 201 ura3-52*) isogenic with strain AA255 (15). The *drs2-1::URA3* strain YR884 was obtained by transformation of YR98 with *drs2-1::URA3* DNA as described below. The *HA::DRS2* strain YR886 carrying an in-frame insertion of 27 base pairs encoding the HA epitope (16) was constructed by transforming YR884 with *HA::DRS2* DNA as described below. All media were prepared according to standard protocols (17).

Construction of drs2-1::URA3 and HA::DRS2 Alleles—To construct *drs2-1::URA3*, the 5.9-kb *EcoRI* fragment carrying the entire *DRS2* gene was isolated from a *DRS2*-containing plasmid (a gift from J. Woolford) and subcloned into pUC19 (18). Subsequently, the 3.5-kb *BstEII-HpaI* fragment within the *DRS2* ORF was replaced with *URA3* sequences by inserting the 1.1-kb *HindIII* fragment of *URA3* via blunt-end ligation. DNA from the resulting plasmid was digested with *EcoRI* and used to transform YR98. The replacement of the *DRS2* gene by *drs2-1::URA3* DNA was verified in one of the Ura⁺ transformants (YR884) by Southern blot analysis.

To obtain the *HA::DRS2* allele, a 27-base pair insertion of HA-encoding DNA (19) was introduced into the 1.1-kb *EcoRI-XhoI* fragment of *DRS2* by joining the polymerase chain reaction products of two independent polymerase chain reaction reactions on a *DRS2* template via recombinant polymerase chain reaction (20). One reaction utilized primers A (5'-ggggccgGAATTCAGCCAAGAGACGTAAG, capital letters indicate bases pairing with the *DRS2* template; the *EcoRI* site is in italics) and B (5'-AGCGTAGTCTGGGACGTCGTATGGGTAATTCATG-GTAAAATCAGGGAATGAAAGAAC, underlined letters correspond to bases encoding the 9-amino acid HA epitope); the other reaction used primers C (5'-TACCCATACGACGTCCCAGACTACGCTGACGACAGAGAAACCCCCCAAAGAGG) and D (5'-CTTATTCTCGAGTCTAG-ATA, *XhoI* site). A mixture of the two reaction products together with primers A and D was used to amplify a recombinant *EcoRI-XhoI DRS2* fragment, which carried the HA DNA inserted between the second and third codon of the *DRS2* open reading frame. To obtain a full-length *HA::DRS2* allele, the recombinant fragment was digested with *CelII* and *XhoI* and subcloned to replace the *CelII-XhoI* fragment within the 5.9 kb of wild-type *DRS2* DNA (*EcoRI-EcoRI*) present in pUC19. For chromosomal integration of *HA::DRS2*, DNA from the resulting plasmid was cut with *EcoRI* and transformed into *drs2-1::URA3* cells together with pRS425, a *LEU2*-containing plasmid. In one of the Leu⁺ transformants (YR886) able to grow at 23 °C like wild type, expression of HA-Drs2p was verified by Western blot analysis.

Vesicle Preparation—P-C₆-NBD-PS, M-C₆-NBD-PE, M-C₆-NBD-PC, DOPC and N-Rh-DOPE were from Avanti Polar Lipids Inc. (Alabaster, AL). Phospholipids were stored at -20 °C, periodically monitored for purity by thin-layer chromatography, and repurified when necessary. Phospholipid concentrations were determined by a lipid phosphorus assay (21). To prepare vesicles, lipids were first mixed in desired proportions, and the chloroform solvent was removed by evaporation under

FIG. 2. Internalization and distribution of P-C₆-NBD-PS and M-C₆-NBD-PE in *drs2-1::URA3* and *DRS2* strains. Cells were grown to early log phase in SDC, washed three times in SDC, and incubated for 30 min at 23 or 30 °C with vesicles containing either P-C₆-NBD-PS or M-C₆-NBD-PE and *N*-Rh-DOPC and DOPC (40:2:58; molar ratio). Cells were washed three times in ice-cold SCN₃ before imaging by fluorescence microscopy as described under "Experimental Procedures." *DIC*, differential interference contrast.



essentially lacking the entire *DRS2* coding sequence. In this *drs2-1::URA3* null allele, the 3.5-kb *Bst*EII-*Hpa*I fragment encoding amino acids 33 to 1206 of the *DRS2* open reading frame was substituted by the yeast *URA3* gene. Transformation of a haploid wild-type strain (YR98) with *drs2-1::URA3* DNA produced the congenic *drs2-1::URA3* strain YR884 used in all subsequent studies. Growth of YR884 was examined on different solid media (yeast extract/peptone/glucose (YPD)), synthetic complete and minimal medium) at 23, 30, and 37 °C. On all media tested, this *drs2-1::URA3* strain grew well at 37 and 30 °C but was unable to grow at 23 °C (data not shown), as reported for the *drs2::TRP1* mutant (23).

Loss of *DRS2* Does Not Alter the Internalization and Distribution of NBD-labeled Aminophospholipids Detected by Fluorescence Microscopy—The internalization and distribution of the NBD-labeled aminophospholipids, P-C₆-NBD-PS and M-C₆-NBD-PE, were observed by fluorescence microscopy in the *drs2-1::URA3* strain and its isogenic *DRS2* parent (Fig. 2). No significant differences were detected between the two strains at 30 °C (permissive for growth) or at 23 °C (nonpermissive for growth). In previous experiments, it was concluded that M-C₆-NBD-PE was internalized exclusively by inward-directed transport across the plasma membrane (flip), resulting in its distribution to the nuclear envelope, endoplasmic reticulum, and mitochondria (24). Internalized M-C₆-NBD-PE was not degraded intracellularly, but was readily transported outward across the plasma membrane (flop), where it was degraded by periplasmic phospholipases (24). The similar pattern of fluorescence distribution observed for P-C₆-NBD-PS and M-C₆-NBD-PE (Fig. 2) suggests that both of these aminophospholipids are internalized and distributed by similar mechanisms in both the *drs2-1::URA3* and *DRS2* strains.

To address the possibility that P-C₆-NBD-PS was internalized by endocytosis, Tang *et al.* (12) labeled *drs2Δ* cells with high concentrations of probe solubilized in Me₂SO incubated on ice to inhibit endocytosis (12). Using our standard protocol to label cells on ice with P-C₆-NBD-PS and M-C₆-NBD-PE incorporated into liposomes resulted in no detectable fluorescence internalization using the sensitive SIT camera to capture images on the fluorescence microscope. We therefore followed the Tang *et al.* protocol for labeling cells on ice using high concentrations of Me₂SO-solubilized NBD-lipids. Following this labeling protocol, no P-C₆-NBD-PS fluorescence could be detected. However, a very low level of M-C₆-NBD-PE fluorescence was detected, but no differences were observed between the

drs2-1::URA3 and *DRS2* strains. Although detectable with the SIT camera, the fluorescence was too faint and diffuse to produce publishable images.

Thus, for all labeling conditions in which detectable amounts of NBD-aminophospholipids were obtained, the loss of Drs2p had no effect on their internalization and distribution. These observations are inconsistent with the previous study in which P-C₆-NBD-PS internalization was abolished in a *drs2* mutant strain (12). The previous conclusion by Tang *et al.* (12) about the function of Drs2p was based on "back exchange" experiments and was not confirmed by direct observation of internalization and distribution by fluorescence microscopy. In the back exchange measurement, inward-directed transport (flip) is inferred from the amount of NBD-phospholipid that cannot be extracted from the surface of labeled cells by incubation with bovine serum albumin. This technique has been used successfully for many years to assay NBD-phospholipid transport in blood cells and reconstituted vesicles (1, 25). However, the report by Tang *et al.* (12) was the first use of back exchange to measure flip in yeast, and in the absence of proper controls, differences in the amount of NBD-phospholipid aggregates sticking to the cell wall or trapped in the periplasm or differences in the rate of NBD-phospholipid hydrolysis by periplasmic phospholipases may have been misinterpreted as differences in inward translocation. Direct observation of NBD-phospholipid internalization by fluorescence microscopy is not subject to these artifacts. One of the advantages of labeling cells with liposomes containing trace amounts of *N*-Rh-DOPC is that the rhodamine fluorescence can be used to determine the extent of cell-associated NBD fluorescence resulting from stuck vesicles (26, 24). This is not possible when cells are labeled with Me₂SO-solubilized NBD-phospholipids.

Quantification of NBD-labeled Phospholipid Accumulation by Flow Cytometry—To make a more quantitative evaluation of the results obtained by fluorescence microscopy, cells were labeled with either P-C₆-NBD-PS, M-C₆-NBD-PE, or M-C₆-NBD-PC, and the average cell-associated NBD fluorescence per cell was obtained by flow cytometry. Fluorescent lipid accumulation was measured for *drs2-1::URA3* and *DRS2* strains grown at 30 °C in two different media (YPAD and SDC). Accumulation of the three NBD-phospholipids was compared at 30° and 23 °C, the nonpermissive growth temperature for *drs2-1::URA3*. The ratio of the cell-associated fluorescence in *drs2-1::URA3* to that of *DRS2* is presented in Table I for the two temperatures and growth media. Similar results were ob-

TABLE I
Percent NBD-phospholipid accumulation of *drs2-1::URA3* strain relative to isogenic parent

Fluorescence accumulation was measured by flow cytometry. A fluorescence intensity histogram was plotted for ~10,000 live cells, and the means and S.D. were calculated for each strain under the appropriate conditions. The percent average accumulation for the Δ *drs2* strain relative to its isogenic parent is presented \pm S.D. The number of independent experiments (*n*) is in parenthesis. For those experiments with an *n* of 2, the mean \pm the range is presented.

NBD-phospholipid	Growth media ^a	Labeling temperature ^b	
		30 °C	23 °C
P-C ₆ -NBD-PS	YPAD	51.3 \pm 18.7 (5)	53.7 \pm 20.8 (5)
	SDC	116.3 \pm 15.4 (3)	118.6 \pm 37.2 (3)
M-C ₆ -NBD-PE	YPAD	70.6 \pm 19.6 (5)	58.6 \pm 17.1 (5)
	SDC	71.4 (1)	70.5 (1)
M-C ₆ -NBD-PC	YPAD	66.4 \pm 7.8 (2)	56.1 \pm 8.3 (2)

^a Cells were grown to early log phase in either YPAD or SDC at 30 °C.

^b Cells were labeled by incubation with donor vesicles containing the appropriate NBD-phospholipid for 30 min at the stated temperature before washing 3 times with SDC/NaN₃.

tained for the two strains and growth media at 30 and 23 °C. However, the results differed dramatically depending on the growth media. For cells grown in YPAD, the NBD fluorescence in the null strain *versus* its parent was decreased from ~30 and 50% for the two NBD-aminophospholipids as well as the choline lipid, M-C₆-NBD-PC. On the other hand, for cells grown in SDC, the null strains actually accumulated ~16% more P-C₆-NBD-PS but ~30% less M-C₆-NBD-PE. The reduction in P-C₆-NBD-PS and M-C₆-NBD-PE internalization observed for cells grown in YPAD is consistent with the interpretation that Drs2p is an aminophospholipid translocase responsible for 30 to 50% that of the internalization measured in the parent strain. However, given the similar reduction in M-C₆-NBD-PC internalization, one would have to surmise that Drs2p was not functionally homologous to its mammalian counterpart in its ability to discriminate between amino and choline head groups. On the other hand, the observation that P-C₆-NBD-PS internalization is actually increased in cells lacking Drs2p grown in SDC does not support the conclusion that Drs2p is an aminophospholipid translocase. It is conceivable that *drs2-1::URA3* cells grown in SDC up-regulate a functional homologue that overcompensates for P-C₆-NBD-PS but not for M-C₆-NBD-PE internalization. A more likely interpretation is that the absence of Drs2p indirectly alters the NBD-phospholipid internalization.

The average cell-associated fluorescence resulting from identical labeling procedures is highly dependent on the strain and the stage of growth. In unpublished experiments,² M-C₆-NBD-PE accumulation varied as much as 10-fold between different wild-type laboratory strains. Furthermore, its accumulation was dramatically reduced in cells allowed to grow to mid-log (optical density >1.0).³ Thus, isogenic backgrounds and identical growth conditions are essential for meaningful comparisons between strains to be made. The existence of unidentified regulatory mechanisms that control the extent of NBD-phospholipid internalization provides a means by which the loss of *DRS2* could indirectly decrease NBD-lipid internalization.

Loss of Drs2p Does Not Alter the Amount of Endogenous Aminophospholipid in the Outer Leaflet of the Plasma Membrane—The amount of endogenous PS and PE in the outer leaflet of the plasma membrane of *drs2-1::URA3* and *DRS2* strains was measured by TNBS labeling. No significant differences were observed in the percent of total PS or PE exposed to the outer leaflet between the two strains. Very little (<0.5%) of the total cellular PS was exposed to the outer leaflet, making it

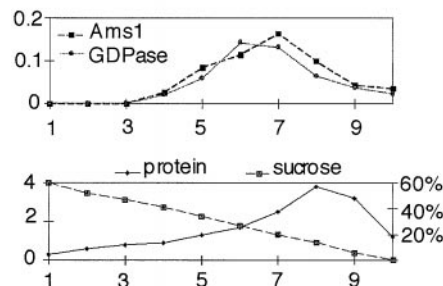
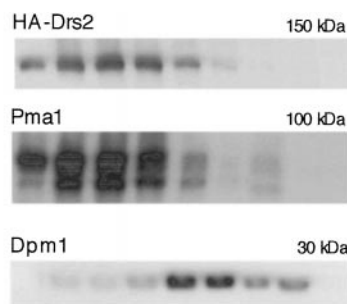


FIG. 3. **Fractionation of HA-Drs2p on sucrose gradients.** Whole cell extracts of the *HA::DRS2* strain YR886 were fractionated by density centrifugation as described (38). Aliquots of the gradient fractions were separated by SDS-polyacrylamide gel electrophoresis and analyzed by Western blotting with anti-HA antibodies, anti-Pma1 antibodies, and anti-Dpm1 antibodies. The sizes of marker proteins are given in kDa; the fraction numbers are indicated. Activities for α -mannosidase (*Ams1*) (32) and guanosine diphosphatase (31) were determined as described and are given in arbitrary units. Density (% sucrose, w/w) and protein concentration (arbitrary units) are plotted against the fraction number.

difficult to detect; however, no measurable differences were observed between the two strains. A readily detectable and reproducible amount of PE was labeled by TNBS. The percentage of total cellular PE exposed to the outer leaflet of the plasma membrane was 1.4 ± 0.3 for the *drs2-1::URA3* strain and 1.6 ± 0.4 for the isogenic *DRS2* parent strain. Thus, the loss of Drs2p had no significant effect on the amount of PE or PS residing in the outer leaflet of the plasma membrane.

Drs2p Localizes to the Plasma Membrane—To facilitate detection of the Drs2p protein, we constructed a derivative of the *DRS2* gene, *HA::DRS2*, harboring a 27-base pair sequence encoding the nine amino acid HA epitope (16, 19) inserted in-frame after the second *DRS2* codon (see Fig. 1). Haploid strain YR886 containing *HA::DRS2* at the chromosomal *DRS2* locus grew indistinguishable from *DRS2* strains, indicating that the expressed HA-Drs2p protein was fully functional (data not shown). To determine the subcellular localization of HA-Drs2p, extracts from strain YR886 (*HA::DRS2*) were fractionated by sucrose gradient centrifugation. All fractions collected from the gradients were tested by SDS-polyacrylamide gel electrophoresis and Western blotting for the presence of marker proteins specific for plasma membrane (H^+ -ATPase Pma1 (27)) and endoplasmic reticulum (dolichol phosphate mannosyl synthase Dpm1 (28–30)). Golgi and vacuolar membranes were identified by monitoring activities of GDPase (31) and α -mannosidase, *Ams1* (32), respectively. As demonstrated by the data shown in Fig. 3, the bulk of HA-Drs2p co-fractionated with the plasma membrane ATPase, well separated from endoplasmic reticulum membranes and the bulk of GDPase or α -mannosidase activity. Consistent with this observations, cells expressing HA-Drs2p from the chromosomal locus exhibited in indirect immunofluorescence microscopy a ring-shaped rim staining pattern, but unfortunately the signal was very low (data not shown). Attempts to increase expression of HA-Drs2p from a

² A. Grant and J. Nichols, unpublished data.

³ P. K. Hanson and J. Nichols, unpublished observation.

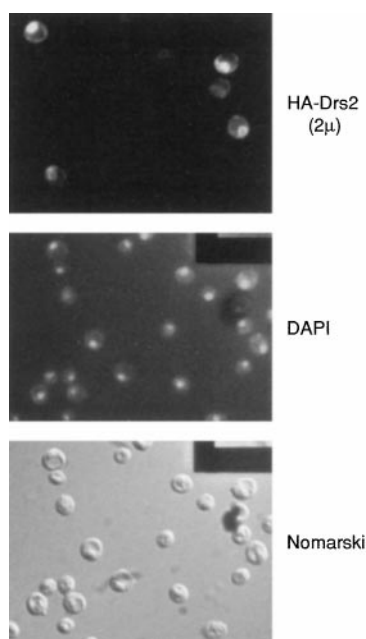


FIG. 4. HA-Drs2p accumulates in the endoplasmic reticulum upon overexpression. Cells expressing carrying the *HA::DRS2* allele on a 2 μ m (μ)-based multicopy plasmid were analyzed for the presence of HA-Drs2p by indirect immunofluorescence (top panel) as described (39). 4',6-Diamidino-2-phenylindole dihydrochloride (DAPI) staining was used to visualize DNA (middle panel). The bottom panel shows the same field using Nomarski optics.

multicopy plasmid yielded a more pronounced rim staining but, in addition, produced a prominent perinuclear staining pattern, suggesting that the bulk of HA-Drs2p remained in the endoplasmic reticulum under these conditions (Fig. 4). Taken together, our data strongly argue for a steady-state localization of Drs2p in the plasma membrane but indicate that Drs2p could also exert functions in membranes of secretory organelles along the pathway to the plasma membrane.

The Steady-state Level of Drs2p Is Dependent on Growth Phase and Temperature—In monitoring expression of HA-Drs2p in *HA::DRS2* cells growing in YPD medium at 30 °C, we found a substantial alteration of the steady-state level of HA-Drs2p with the growth phase of the culture. Fig. 5A (top panel) shows a Western blot analysis of crude membranes prepared from *HA::DRS2* cells at various stages of growth (A_{600} of 0.6, 1.1, and 2.0). HA-Drs2p was fairly abundant during early and mid logarithmic growth but essentially disappeared as cells entered stationary phase. In contrast, the steady-state level of the plasma membrane H^+ -ATPase (Pma1p), which like Drs2p, is a member of the P-type ATPase family, did not show such a dramatic decrease, although Pma1p appeared somewhat reduced in cells approaching stationary phase (Fig. 5A, bottom panel). However, as demonstrated in Fig. 5B, cells entering stationary phase while growing at 23 °C retained a substantial amount of HA-Drs2p. This finding was consistent with the observed requirement of *DRS2* for growth at this temperature (23). Taken together, these data suggested an important function for Drs2p, particularly during early growth phases at 30 °C and during growth at lower temperatures.

The Steady-state Level of Drs2p Increases upon Treatment with Heavy Metals—In the course of our genetic analysis, we discovered a hypersensitivity of *drs2-1::URA3* mutants toward various heavy metals. As displayed in Fig. 6, serial dilutions of a *drs2-1::URA3* culture were spotted onto solid minimal media containing the indicated concentrations of manganese (II), cobalt (II), nickel (II), or zinc (II) chloride. Evidently, the *drs2-1::URA3* strain was particularly sensitive to Zn^{2+} and

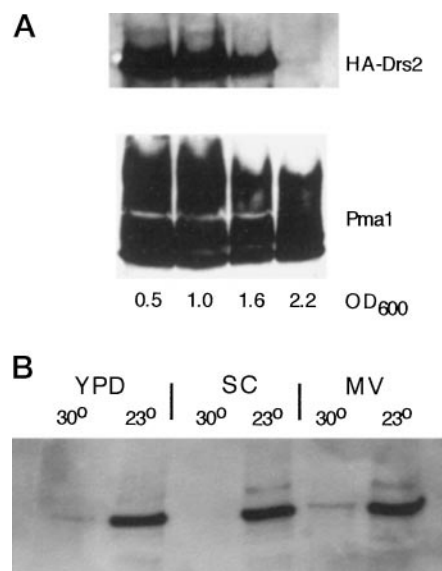


FIG. 5. Alteration of the HA-Drs2p steady-state level with growth phase and temperature. Panel A, aliquots were withdrawn from a *HA::DRS2* culture (YR886) in YPD at various optical densities (A_{600}) as indicated. Crude membranes were prepared as described (39) and analyzed for the presence of HA-Drs2p by Western blotting (top). The blot was then stripped and reprobed for the presence of Pma1 (bottom) as described (39). Each lane corresponds to 12 absorbance units of cells. Panel B, *HA::DRS2* cultures were grown into stationary phase in rich (YPD), synthetic complete (SC), and minimal (MV) media at 30 and 23 °C. The amount of HA-Drs2p present under these conditions was analyzed as in panel A. Each lane corresponds to 30 μ g of total protein.

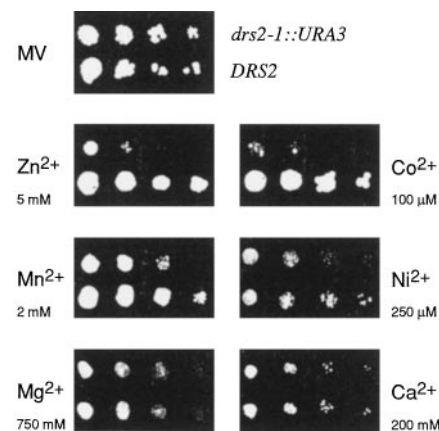


FIG. 6. Hypersensitivity of the *drs2-1::URA3* mutant against heavy metals. Serial 10-fold dilutions of a saturated culture of *drs2-1::URA3* cells (YR884) grown in minimal medium were spotted onto regular minimal medium (MV) and on MV plates containing the indicated amounts of divalent cations added as chlorides. Plates were photographed after 3 days of incubation at 30 °C.

Co^{2+} , and the hypersensitivity toward Mn^{2+} and Ni^{2+} was less pronounced. This growth inhibition by divalent cations was apparently restricted to transition elements, because *drs2-1::URA3* grew like wild type in the presence of high concentrations of Mg^{2+} and Ca^{2+} (see Fig. 6).

We also examined the steady-state levels of HA-Drs2p accumulating in cells during growth in the presence of various metal cations. To this end, *HA::DRS2* cells were inoculated into YPD media to which the indicated amounts of metal chlorides have been added. At an A_{600} of 0.6, 1.1, and 2.0, aliquots were withdrawn and analyzed for the presence of HA-Drs2p in crude membrane fractions. As seen in Fig. 7, all cations inhibitory to growth, *i.e.* Co^{2+} , Ni^{2+} , Mn^{2+} , and Zn^{2+} , also led to a pronounced accumulation of HA-Drs2p relative to the

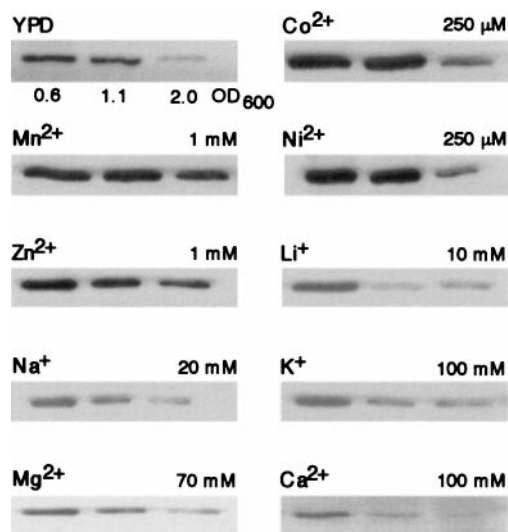


FIG. 7. Accumulation of HA-Drs2p upon treatment with divalent heavy metals. YR886 cells (*HA::DRS2*) were grown in regular rich medium (YPD) and in YPD media supplemented with the indicated amounts of metal chlorides. At an optical density (A_{600}) of 0.6, 1.1, and 2.0, respectively, aliquots were withdrawn and analyzed for the presence of HA-Drs2p in crude membrane preparations as described in Fig. 5. Each lane corresponds to 30 μ g of total protein.

control culture. In contrast, the presence of Mg^{2+} , Ca^{2+} , or monovalent cations had only slight effects on the steady-state level of HA-Drs2p. Both observations, the hypersensitivity of *drs2-1::URA3* cells to heavy metals and the intracellular accumulation of HA-Drs2p triggered by the same divalent cations, indicated that cells required Drs2p function to effectively endure the toxic effects of these transition elements.

DISCUSSION

The current knowledge about the mechanisms leading to internalization of phospholipids into the yeast *S. cerevisiae* stems primarily from studies utilizing phospholipid molecules carrying one short acyl chain labeled with a fluorescent NBD group. Digital, video-enhanced fluorescence microscopy and spectrofluorometry have shown that at least two distinct pathways for phospholipid internalization exist: 1) transport by endocytosis to the vacuole, which partially accounts for the uptake of the NBD-labeled PC analog, M-C₆-NBD-PC (26) and 2) transport by a nonendocytic pathway to the nuclear envelope and mitochondria. This route accounts for the remainder of the M-C₆-NBD-PC internalization, whereas the NBD-labeled analogs of the aminophospholipids, M-C₆-NBD-PE (24) or P-C₆-NBD-PS (33), appear to be exclusively internalized via this pathway. Based on the inhibition of M-C₆-NBD-PE uptake by treatment with NEM at low temperature, this pathway is thought to involve a protein-mediated translocation of phospholipids from the outer to the inner leaflet of the plasma membrane (24). Because these NBD-labeled aminophospholipids are more water-soluble than their endogenous counterparts (34), they most likely spontaneously redistribute between the inner leaflet of the plasma membrane and membranes of other intracellular organelles. Because cells are also able to translocate M-C₆-NBD-PE outward across the plasma membrane (24), the extent of intracellular accumulation depends on the steady-state distribution of the NBD-labeled phospholipid established between the inner and outer leaflets of the plasma membrane by the coordinate regulation of the influx and efflux pathways. As a result, the extent of intracellular accumulation can be considered to be an amplification of the steady-state amount of the NBD-labeled aminophospholipid residing in the inner leaflet that is established by the regulation of the influx and efflux

pathways. This view is corroborated by the analysis of *pdr1-11* and *pdr3-11* mutant strains, in which the net influx of M-C₆-NBD-PE is reduced from 50- to 100-fold. These strains also exhibited a three to four-fold increase in the amount of endogenous PE residing in the outer leaflet of the plasma membrane (24). In this case, a decrease in the intracellular accumulation of M-C₆-NBD-PE correlated with an increase in the amount of endogenous PE residing in the outer leaflet of the plasma membrane.

Given the identification of *DRS2* as the exclusive or at least major functional aminophospholipid transporter in the plasma membrane of *S. cerevisiae* (12), we compared the intracellular accumulation of P-C₆-NBD-PS and M-C₆-NBD-PE as well as the percent of TNBS-labeled PS and PE in the outer leaflet of the plasma membrane between a *drs2-1::URA3* mutant strain and its isogenic *DRS2* parent. The deletion of the *DRS2* gene had no effect on the internalization and distribution of P-C₆-NBD-PS and M-C₆-NBD-PE detected by fluorescence imaging, nor did the deletion have a measurable effect on the distribution of endogenous PS and PE across the plasma membrane. Quantitation of the extent of accumulation by a large population of cells (~10,000 live cells) indicated that the deletion of the *DRS2* gene resulted in a significant decrease in P-C₆-NBD-PS, M-C₆-NBD-PE, and M-C₆-NBD-PC accumulation following growth in YPAD at 30 and 23 °C. However, the decrease of P-C₆-NBD-PS accumulation was completely reversed in cells grown in SDC. The mean accumulation of M-C₆-NBD-PE was decreased in *drs2-1::URA3* cells grown in both media. Thus, the observed decrease in NBD-phospholipid internalization in the *drs2* null strain was dependent on the growth media and was not exclusive to the aminophospholipids.

These data definitively exclude the possibility that Drs2p is the exclusive or major aminophospholipid translocase in the plasma membrane of *S. cerevisiae*. However, these negative results do not exclude the possibility that Drs2p functions as a phospholipid translocase in intracellular membranes or is one of several plasma membrane aminophospholipid translocases. In the latter case, the partial loss of aminophospholipid internalization in the *drs2* strain would be compensated by additional transporters under the appropriate growth conditions. Interestingly, *DRS2* and four yeast homologs form a distinct subgroup, cluster II, within the P-type ATPase family (13). These four homologs have no known function and are potential candidates to code for additional aminophospholipid transporters. However, because of the complex nature of the regulation of aminophospholipid transport across the plasma membrane and its dependence on growth conditions, one cannot exclude from the data presented that the observed alterations in P-C₆-NBD-PS and M-C₆-NBD-PE accumulation in the *drs2-1::URA3* null strain are secondary to other effects on growth or some other cellular function.

At present, the mechanisms leading to the observed hypersensitivity of a *drs2* null mutant toward some heavy metal cations, in particular Zn^{2+} , Co^{2+} , Mn^{2+} , and Ni^{2+} , are not known. In our view, these phenotypes could either reflect a yet undiscovered role of Drs2p as a transporter of divalent cations or are indeed a consequence of the proposed function of Drs2p in aminophospholipid translocation. Two models, not necessarily exclusive, could provide an explanation for a link between aminophospholipid translocation and cation sensitivity. (i) An altered asymmetric distribution of lipids within some cellular membranes, presumably resulting from the loss of Drs2p, could compromise the activity of cation transporters embedded in the affected membranes. Given a prominent localization of Drs2p in the plasma membrane and the numerous exocytic and endocytic pathways leading to and originating from this mem-

brane, it seems possible that Drs2p function might impinge upon Golgi and vacuolar membranes, which both harbor numerous transport proteins engaged in the sequestration of divalent cations within these organelles. (ii) Alternatively, an altered lipid distribution, *i.e.* a reduction in the amount of negatively charged PS in the cytoplasmic leaflets of some intracellular membranes, might directly result in altered cation binding properties of these membranes, thereby affecting some cation-dependent steps in membrane fusion reactions. Noteworthy, *in vitro* studies have shown that Zn²⁺ ions are more effective than Ca²⁺ to induce fusion of phospholipid vesicles with a low content of PS (35), and the depletion of Zn²⁺ blocks endosome fusion in a cell-free system (36).

It should be noted that the loss of Drs2p function also impairs ribosome biogenesis. The *DRS2* gene was first discovered in a search for mutants with an altered ratio of free 40 to 60 S ribosomal subunits or qualitative changes in polyribosome profiles. The *drs2* mutant isolated in this screen processes the 20 S precursor of the mature 18 S rRNA slowly and is deficient in 40 S ribosomal subunits (23). It has been demonstrated that a block in the secretory pathway, which can readily be introduced at different stages of the pathway through the use of conditional alleles in various *SEC* genes absolutely required for secretion, leads to the rapid shut-down of ribosome biogenesis. Thus, the continuous functioning of the secretory pathway appears to be a prerequisite for the biogenesis of ribosomes (37). Evidently, the proposed role for Drs2p as a flippase affecting lipid distribution in vesicles of the late secretory pathway or at the plasma membrane would provide an intriguing explanation for the ribosome-related defects observed in the *drs2* mutant (23).

Finally, we would like to emphasize that the previous demonstration of the abolishment of PS internalization in a yeast *drs2* mutant (12) provided the sole functional data for the assignment of phospholipid translocase activity to the Drs2p subfamily within the class of P2 ATPases (13). Our inability to confirm a role of Drs2p in phospholipid translocation underscores the need for future experiments to carefully reevaluate this functional assignment.

Acknowledgments—We thank Tracy Ripmaster and John Woolford for providing *DRS2* plasmids and yeast strains and Ralf Egner and Karl Kuchler for antibodies and advice on subcellular fractionation.

REFERENCES

1. Devaux, P. F. (1991) *Biochemistry* **30**, 1163–1173
2. Diaz, C., and Schroit, A. J. (1996) *J. Membr. Biol.* **151**, 1–9

3. Williamson, P., and Schlegel, R. A. (1994) *Mol. Membr. Biol.* **11**, 199–216
4. Rosing, J., Tans, G., Govers-Riemslog, J. W., Zwaal, R. F., and Hemker, H. C. (1980) *J. Biol. Chem.* **255**, 274–283
5. Connor, J., Pak, C. C., and Schroit, A. J. (1994) *J. Biol. Chem.* **269**, 2399–2404
6. Fadok, V. A., Savill, J. S., Haslett, C., Bratton, D. L., Doherty, D. E., Campbell, P. A., and Henson, P. M. (1992) *J. Immunol.* **149**, 4029–4035
7. Fadok, V. A., Voelker, D. R., Campbell, P. A., Cohen, J. J., Bratton, D. L., and Henson, P. M. (1992) *J. Immunol.* **148**, 2207–2216
8. Smith, A. J., Timmermans-Hereijgers, J. L., Roelofsens, B., Wirtz, K. W., van Blitterswijk, W. J., Smit, J. J., Schinkel, A. H., and Borst, P. (1994) *FEBS Lett.* **354**, 263–266
9. van Helvoort, A., Smith, A. J., Sprong, H., Fritzsche, I., Schinkel, A. H., Borst, P., and van Meer, G. (1996) *Cell* **87**, 507–517
10. Ruetz, S., and Gros, P. (1994) *Cell* **77**, 1071–1081
11. Decotignies, A., Grant, A. M., Nichols, J. W., de Wet, H., McIntosh, D. B., and Goffeau, A. (1998) *J. Biol. Chem.* **273**, 12612–12622
12. Tang, X., Halleck, M. S., Schlegel, R. A., and Williamson, P. (1996) *Science* **272**, 1495–1497
13. Catty, P., de Kerchove d'Exaerde, A., and Goffeau, A. (1997) *FEBS Lett.* **409**, 325–332
14. Lutsenko, S., and Kaplan, J. H. (1995) *Biochemistry* **34**, 15607–15613
15. Rudolph, H. K., Antebi, A., Fink, G. R., Buckley, C. M., Dorman, T. E., LeVitre, J., Davidow, L. S., Mao, J. I., and Moir, D. T. (1989) *Cell* **58**, 133–145
16. Wilson, I. A., Niman, H. L., Houghten, R. A., Chersonson, A. R., Conolly, M. L., and Lerner, R. A. (1984) *Cell* **37**, 767–778
17. Sherman, F., Fink, G. R., and Hicks, J. (1986) *Methods in Yeast Genetics*, Cold Spring Harbor Laboratory, Cold Spring Harbor, NY
18. Yanisch-Perron, C., Vieira, J., and Messing, J. (1985) *Gene* **33**, 103–119
19. Kolodziej, P. A., and Young, R. A. (1991) *Methods Enzymol.* **194**, 508–519
20. Higuchi, R., Krummel, B., and Saiki, R. K. (1988) *Nucleic Acids Res.* **16**, 7351–7367
21. Ames, B. N., and Dubin, D. T. (1960) *J. Biol. Chem.* **235**, 769–775
22. Marinetti, G. V., and Love, R. (1976) *Chem. Phys. Lipids* **16**, 239–254
23. Ripmaster, T. L., Vaughn, G. P., and Woolford, J. J. (1993) *Mol. Cell. Biol.* **13**, 7901–7912
24. Kean, L. S., Grant, A. M., Angeletti, C., Mahe, Y., Kuchler, K., Fuller, R. S., and Nichols, J. W. (1997) *J. Cell Biol.* **138**, 255–270
25. Schroit, A. J., and Zwaal, R. F. A. (1991) *Biochim. Biophys. Acta* **1071**, 313–329
26. Kean, L. S., Fuller, R. S., and Nichols, J. W. (1993) *J. Cell Biol.* **1403**–1419
27. Serrano, R. (1978) *Mol. Cell. Biochem.* **22**, 51–63
28. Marriott, M., and Tanner, W. (1979) *J. Bacteriol.* **139**, 566–572
29. Czichi, U., and Lennarz, W. J. (1977) *J. Biol. Chem.* **252**, 7901–7904
30. Preuss, D., Mulholland, J., Kaiser, C. A., Orlean, P., Albright, C., Rose, M. D., Robbins, P. W., and Botstein, D. (1991) *Yeast* **7**, 891–911
31. Abeijon, C., Orlean, P., Robbins, P. W., and Hirschberg, C. B. (1989) *Proc Natl Acad Sci U. S. A.* **86**, 6935–6939
32. van der Wilden, W., Matile, P., Schellenberg, M., Meyer, J., and Wiemken, A. (1973) *Z. Naturforsch.* **28**, 416–421
33. Grant A. M. (1998) *An Analysis of the Mechanisms of Phospholipid Transport in S. Cerevisiae*. Ph.D. thesis, Emory University
34. Nichols, J. W. (1985) *Biochemistry* **24**, 6390–6398
35. Barfield, K. D., and Bevan, D. R. (1985) *Biochem. Biophys. Res. Commun.* **128**, 389–395
36. Aballay, A., Sarrouf, M. N., Colombo, M. I., Stahl, P. D., and Mayorga, L. S. (1995) *Biochem. J.* **312**, 919–923
37. Mizuta, K., and Warner, J. R. (1994) *Mol. Cell. Biol.* **14**, 2493–2502
38. Egner, R., Mahe, Y., Pandjaitan, R., and Kuchler, K. (1995) *Mol. Cell. Biol.* **15**, 5879–5887
39. Wieland, J., Nitsche, A. M., Strayle, J., Steiner, H., and Rudolph, H. K. (1995) *EMBO J.* **14**, 3870–3882